SIMILAR SPACING OF BASIN RINGS ON MARS, MERCURY AND THE MOON. R. J. Pike, U. S. Geological Survey, Menlo Park, CA 94025; P. D. Spudis, U. S. Geological Survey, Flagstaff, AZ 86001, and Dept. Geol., Ariz. State U., Tempe, AZ 85287.

A constant radial increment of $(2.0 \pm 0.1)^{-2}D$, where D=ring diameter, separates adjacent rings and arcs of multi-ring basins on Mars, Mercury, and the Moon. The interval seems fundamental to all recognizable basins, not just to a few examples on the Moon such as the well-preserved Orientale [1]. The statistical periodicity is evident now because only recently has the sample of observed basins (64) and rings (279) on the three planets become sufficiently large. Our revised ring diameters come from photogeologic analysis of Viking Orbiter, Lunar Orbiter, and Mariner-10 images and maps. This short paper summarizes current observations, with special emphasis on Mars. A companion note describes lunar and mercurian data, the numerical ranking of basin rings by graphical analysis, and our initial interpretations [2].

We reexamined the martian basins of [3] and [4] on Viking photomaps and mosaics, and mapped 107 rings and arcs for 24 multi-ring basins, a few differing from those of [3,4]. Plotting ring diameters against that of the physiographically strongest ring for each basin in the $\log_{10}$ domain separated the rings into eight linear clusters, six of which are amenable to least-squares analysis (Fig. 1) [2]. Twelve of the 107 rings lie inside rank I or are paired in a single rank. Table 1 gives linear log-log fits for diameters of the main ring (X), D_{IV}, and those of inner and outer rings (Y), $D_{I...VII}$. The results, which include geometric similitude of the peak ring in two-ring basins with ring II in multi-ring basins (not shown), mimic those (updated here in Table 1) obtained previously for the Moon and Mercury [2,5].

Figure 2 summarizes for all 64 multi-ring basins on the three planets the close correspondence of observed ring spacing, $x^{-2}D$, to the hypothesized spacing, $2^{-2}D$. Values of x for ring ranks I-VII were derived from least-squares results (Table 1): Each observed ring ratio ($D_{I...VII}/D_{IV}$; geometric means) was equated with an expression (parenthesized in Fig. 2) containing x so that the model spacing, regardless of ring rank, always = 2.0. For example, because $D_{IV}/D_{IV}=1.0$, the expression must=x/2. For D_V/D_{IV}, which the model predicts to be 1.414 (2^{-2}), the requisite expression=x^{-2}; the observed 1.496 ratio of rings V/IV on Mars, for which x=2.2, exceeds the hypothesized spacing. Mean x for all 18 non-D_{IV}/D_{IV} equations is 2.002 ± 0.104, which confirms that the spacing increment observed for basin rings varies within a narrow range, from 1.9^{-2} to 2.1^{-2}, never far from the hypothesized 2^{-2} of [1].

Figure 2 prompts four further conclusions: (1) There are more interior than exterior rings, with II, III, and V equally frequent. The difference may be observational; (2) Most rings II and VI closely follow the $2^{-2}D$ model whereas rings I and VII scatter more widely about it; (3) Rings III and V both lie farther from ring IV than the 2^{-2} interval, a systematic (and unexplained) symmetry about the main ring; and most importantly (4) Three planets that differ markedly in gravity and other physical properties, crustal structure, and geologic and thermal history all show the same $2^{-2}D$ spacing for basin rings.

The fourth conclusion, above, suggests that the physics of the impact itself directly controls the process(es) of ring formation. We believe that the large amount of energy released in a basin-sized impact overrides all crustal influences and imprints any silicate planet with an invariant ringed signature. Target characteristics, at most, modulate the imprinted concentric geometry; postimpact geologic events only modify the initial ring pattern.

The constant spacing factor suggests physical control of basin ring formation by some periodic wave function. We have proposed that basin rings are structural features formed along concentric zones of stress induced by a standing, rather than a travelling, wave [2]. Our current model has three major attributes: (1) It accounts for numerous geologic observations that associate deep-seated structure with basin rings [6-9]; (2) its increasing spacing (outward) between rings is inconsistent with the constant spacing presumably required by the "tsunami"

traveling-wave mechanism [10,11] (unless ad hoc lithospheric thicknesses are invoked [11]); and (3) it provides the long-sought process link between basins and large complex craters, in that topographic patterns expressed by both features [5] result directly from the impact. Standing-wave propagation requires a wave guide [11]. We propose that such a feature is provided by the "strength crater" [12-14], a dynamic zone of crushed target material created during impact. A remaining enigma: why basin rings are spaced at $2^{-2}D$ and not some other number.

References: [1] Fielder G. (1963) Nature 198, 1256. [2] Pike R. J. and Spudis P. D. (1983) NASA TM, in-press. [3] Schultz P. H. et al. (1982) JGR 87, 9803; Schultz P. H. and Glicken H. (1979) JGR 84, 8033. [4] Wood C. A. (1980) PLPSC 11th, 2221. [5] Pike R. J. (1983) LPS XIV, 610. [6] Hartmann W. and Wood C. (1971) Moon 3, 3. [7] McCauley J. F. (1977) PEPI 15, 220. [8] Schultz P. H. (1976) Moon Morph., 626 pp. [9] Spudis P. D. (1982) Ph.D. Thesis, ASU, 292 pp. [10] Baldwin R. (1981) PLPSC, 12A, 175. [11] Van Dorn W. G. (1968) Nature 220, 1102. [12] Ivanov B. A. (1976) PLSC 7, 2947. [13] Croft S. K. (1981) PLPS 12A, 207. [14] Schultz P. H. et al. (1981) PLPSC 12A, 181.

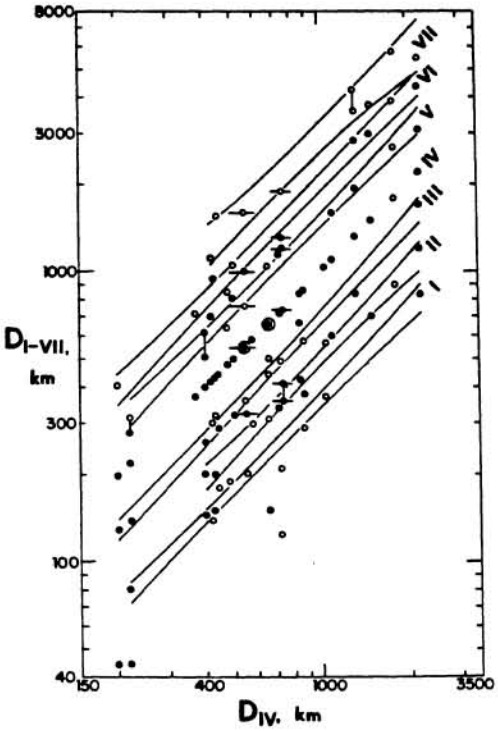

Figure 1. Dots: ring diameter, $D_{I...VII}$, (n=100) as a function of main-ring diameter, D_{IV}, for 24 multi-ring basins on Mars (cf. [2]). Sloping lines are 95% confidence intervals for six resulting clusters of rings (five low "orphan" points, not analyzed statistically, belong to two ranks <I). Accompanying least-squares fits, spaced at roughly $2^{-2}D$ increments, are given in Table 1. Circles are partial arcs, weighted less in the fits. Short vertical lines join two rings that occupy the same rank in one basin; short horizontal lines bracket mean D_{IV} values derived from two or three closely spaced rings.

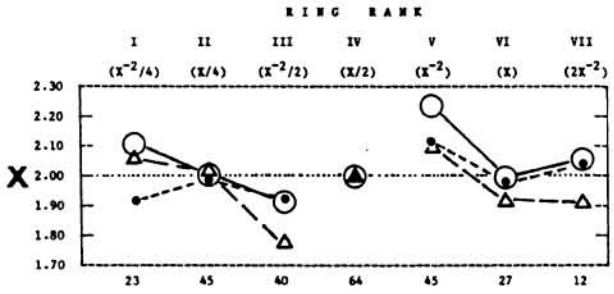

Figure 2. Intervals of radial spacing between $D_{I...VII}$ and D_{IV}, for basin rings on Mars (○), Moon (●), and Mercury (△), expressed as values of x, where $D_{I...VII}/D_{IV}$ = the parenthesized expressions containing x such that x = 2.0 if the rings are spaced at exactly the $2^{-2}D$ interval. See text. Number of occupied ring positions, on all three planets, at bottom.

Table 1. Theoretical and Observed Ring Spacing for Three Planets

Rings (least-squares fits)	n	r	Slope	$D_{I...VII}$ at D_{IV}=1.0 (km)	Ring Ratio $D_{I...VII}/D_{IV}$* (Theor.)	(Obs.)	x see text
			MARS				
I/IV	10	0.996	1.013	0.332	0.354	0.363	2.103
II/IV	14	0.989	1.026	0.421	0.500	0.503	2.011
III/IV	15	0.995	1.058	0.474	0.707	0.691	1.910
IV/IV	24	--	1.000	--	1.000	--	2.000
V/IV	13	0.994	1.002	1.472	1.414	1.496	2.238
VI/IV	11	0.995	1.018	1.772	2.000	1.990	1.990
VII/IV	8	0.983	0.948	4.106	2.828	2.865	2.052
			MERCURY				
I/IV	7	0.843	0.858	0.949	0.354	0.359	2.058
II/IV	15	0.992	1.069	0.322	0.500	0.504	2.018
III/IV	12	0.985	1.155	0.235	0.707	0.666	1.775
IV/IV	23	--	1.000	--	1.000	--	2.000
V/IV	18	0.986	0.932	2.245	1.414	1.448	2.097
VI/IV	9	0.994	1.040	1.477	2.000	1.915	1.915
VII/IV	1	--	--	--	2.828	(2.76)	(1.91)
			MOON				
I/IV	6	0.972	0.982	0.390	0.354	0.347	1.927
II/IV	15	0.986	0.906	0.909	0.500	0.497	1.989
III/IV	13	0.990	1.005	0.671	0.707	0.693	1.919
IV/IV	17	--	1.000	--	1.000	--	2.000
V/IV	14	0.991	1.020	1.276	1.414	1.451	2.106
VI/IV	7	0.993	1.019	1.753	2.000	1.975	1.975
VII/IV	3	0.999	0.95	3.97	2.828	2.86	2.04

* Geometric means